SURF Progress Report 1: The effect of orbital eccentricity in binary black hole simulations on gravitational waveforms

Halston Lim, California Institute of Technology*
Mark Scheel, SURF Mentor

August 15, 2016

1 Background

1.1 Binary Black Holes and Gravitational Waves

The theory of General Relativity predicts gravitational wave (GW) emission from binary systems consisting of compact objects such as neutron stars and stellar mass black holes (BH). This prediction was recently verified by the Laser Interferometer Gravitational-Wave Observatory (LIGO), which detected GW emission from several binary black hole (BBH) mergers [1]. Once detected, such GW signals can be used to infer source information, such as mass ratios and spins, by a process known as parameter estimation. However, the detection of GWs relies on high quality, accurate theoretical waveforms. Such waveforms can be either computed with analytical approximations such as post-Newtonian theory (PN) or calculated directly by numerically solving the full set of Einstein's equations.

For isolated systems, the orbit of a compact binary system will gradually become circular due to gravitational wave emission. When the GWs reach detection frequency, the eccentricity is expected to be negligible [2], and therefore only circular waveforms are used to search for GW signals in LIGO data. Since the PN approximation is a perturbative solution which solves Einstein's equations in powers of v/c, when objects are very close together (and $v/c << 1$ is not necessarily true), the PN waveforms are no longer accurate. In these strong field regimes, numerical relativity can provide a solution with an accuracy limited only by available computational resources.

Unlike PN theory, in the full relativistic theory, the initial velocities corresponding to a quasi-circular orbit cannot be computed in closed form. One way to determine these velocities is to start with a reasonable guess, run a simulation long enough to measure the eccentricity, and then compute an updated guess. This is currently implemented in the Spectral Einstein Code (SpEC), a multi-domain pseudo-spectral evolution code originally developed by Lawrence Kidder, Harald Pfeiffer, and Mark Scheel, that, given initial spins and a mass ratio, calculates inspiral orbits, merger, and ringdown of

*This SURF project will be sponsored by the Mellon Mays Undergraduate Fellowship Program.

compact binaries [3, 4].

The GWs emitted from eccentric binaries are expected to be different from non-eccentric (circular) binaries - namely, the frequency content of eccentric waveforms is more complicated than that of non-eccentric ones [5]. Also, the peak emitted power will be greater due to a greater orbital apastron, leading to more dynamical motion. Therefore, if the BBHs LIGO detects are truly circular, then numerical relativity waveforms should also derive from *effectively* circular orbits. Since the eccentricity reduction scheme used by SpEC results in orbits that have $e \approx 10^{-4}$, it is important to determine how small the eccentricity of a numerical relativity simulation must be in order to justify treating it as zero.

2 Research Goals

The primary objectives of this SURF project are:

- First, to determine the effect of eccentricity on the GW emission from BBHs and to compare the properties of the waveforms using some distinguishability criteria.
- Second, to investigate the experimental implications of using eccentric waveforms on detection and parameter estimation. We will aim to determine the smallest orbital eccentricity required in order to be experimentally indistinguishable from zero eccentricity.
- Third, to learn about the computational techniques used in numerical relativity. More specifically, to gain experience with the SpEC evolution code in application to BBH inspirals.

3 Recent Progress

3.1 Preparing Simulations in BFI

The effect of eccentricity on the GW signal can be deduced by comparing waveforms from BBHs that share the same spins and masses, but differ in eccentricity. Before generating any of these simulations on our own, we checked the Simulation Annex, a catalog of all the completed simulations in SpEC, which also includes their relevant parameters (spins, masses, eccentricities) [6, 7]. Only one set of the existing simulations matched the criteria: the "EccSeries_q3" set comprises of four non spinning simulations, each with mass ratio of $q = 3$ and eccentricities summarized in the table below:

Name	e
Ecc0	0.0197
Ecc1	0.00888
Ecc2	0.00639
Ecc3	0.00628

Table 1: Summary of completed SpEC runs in "EccSeries_q3" which will be used in this project.

For the remaining simulations we adpated the iterative eccentricity reducing scheme, already coded into SpEC, to generate full simulations of similar mass and spins but with varying eccentricity [8]. For each iteration, SpEC first evolves the system a few orbits, then extrapolates the eccentricity and adjusts the initial separation of the BHs, the initial time derivative of the separation, and the orbital frequency such that the next iteration has a smaller resulting eccentricity, until the eccentricity is less than some target (typically 10^{-4}) or fails to decrease with successive iterations [9]. For the first iteration, the user can calculate approximate initial parameters using the PN formalism.

To make the eccentricity reducing scheme applicable to our project, instead of evolving the iterative simulations for only $2-3$ orbits, we will allow these simulations to run to completion in order to extract the gravitational wave signal. This way, for a given BBH system, a range of eccentricities can be generated without implementing significant changes to the code.

To start the SpEC simulation, relevant info files containing the mass, spin, and initial data of the system must be submitted as a job to a computer cluster, in our case the Zwicky cluster run by the SXS collaboration. To organize and simplify this process, especially when multiple jobs need to be monitored, we used the Binary Factory Infrastructure, developed by Dan Hemberger. Below is a table which summarizes the simulations which we submitted and are currently in progress:

Name	q	$\|\chi^A\|$	χ^A_θ	χ^A_ϕ	$\|\chi^B\|$	χ^B_θ	χ^B_ϕ
7.1	3.0	0.7	0	0	0.6	0	0
7.2	3.0	0.7	3.14159	0	0.6	3.14159	0
7.3	3.0	0.7	1.0	0.5	0.6	0.5	1.0
7.4	3.0	0.7	1.0	0.5	0.6	2.0	4.0
7.5	2.0	0.0	0.0	0.0	0.0	0.0	0.0
7.6	1.0	0.0	0.0	0.0	0.0	0.0	0.0

Table 2: Summary of SpEC runs currently in progress. Here, q is the mass ratio and χ^X_μ is the μ-component of the initial spin vector for black hole X. Given the magnitude of the spin vector, $|\chi^X|$, and two components $\chi^X_\theta, \chi^X_\phi$, the third can be determined.

During the first week of SURF, we generated a script which uses the SpEC output of the six listed jobs (using the normal eccentricity reduction scheme) in table 2 and prepares the six jobs for a modified eccentricity reduction, where each iteration is evolved to completion. Including "EccSeries_q3", there are in total seven BBH systems of unique mass and spins, and for each case, several orbits with different eccentricities to compare between. We should not only be able to determine the effect of eccentricity on the waveform, but also how that effect changes with mass ratio, and spin (no spin, aligned spin, or precessing spin case).

3.2 Comparing Waveforms and GWFrames

During the second and third week, we worked on comparing waveforms. The module *GWFrames* contains many useful operations on time series waveforms including noise weighted inner products, derivatives, and fourier transforms [10]. For this SURF project, we utilize a match function, which, given two waveforms expressed in the frequency domain, outputs the maximum inner product, optimized over extrinsic parameters (relative time and phase of coalescence) and normalized. The match between two waveforms u_1, u_2 is expressed as:

$$\text{Match}(u_1, u_2) = \max_{t_c, \phi_c} \langle u_1 | u_2 e^{i(2\pi f t_c - \phi_c}\rangle, \tag{3.1}$$

where the inner product $\langle x|y\rangle$ can be calculated with the Fourier transforms, $\tilde{x}(f)$ and $\tilde{y}^*(f)$, where $*$ denotes the complex conjugate:

$$\langle x|y\rangle = 4\text{Re}\int_0^\infty \frac{\tilde{x}(f)\tilde{y}^*(f)}{S_n(f)} df. \tag{3.2}$$

Here, $S_n(F)$ is the strain noise power spectral density of the interferometer, which can determined by measuring the noise over a long period of time, and computing the Fourier transform, $\mathscr{F}[n(t)] = \tilde{n}(f)$:

$$\langle \tilde{n}(f)\tilde{n}^*(f')\rangle = \frac{1}{2}\delta(f-f')S_n(f) \tag{3.3}$$

SpEC calculates the entire GW emission, so the complex waveforms can either represent one specific spherical harmonic mode, (need to specify l and m), or represent the total signal with all modes but in a particular direction (requires a specific direction of propogation with respect to the BBH inertial coordinates: (θ,ϕ)). For BBHs, most of the GW energy is in the $(2,2)$ mode. Figure 1 plots the mismatch between each waveform in the "EccSeries_q3" (Ecc0,Ecc1,Ecc2,Ecc3), and the most circular, Ecc3. Based on figure 1, the mismatch due to eccentricity is the greatest for BBHs oriented edge-on and

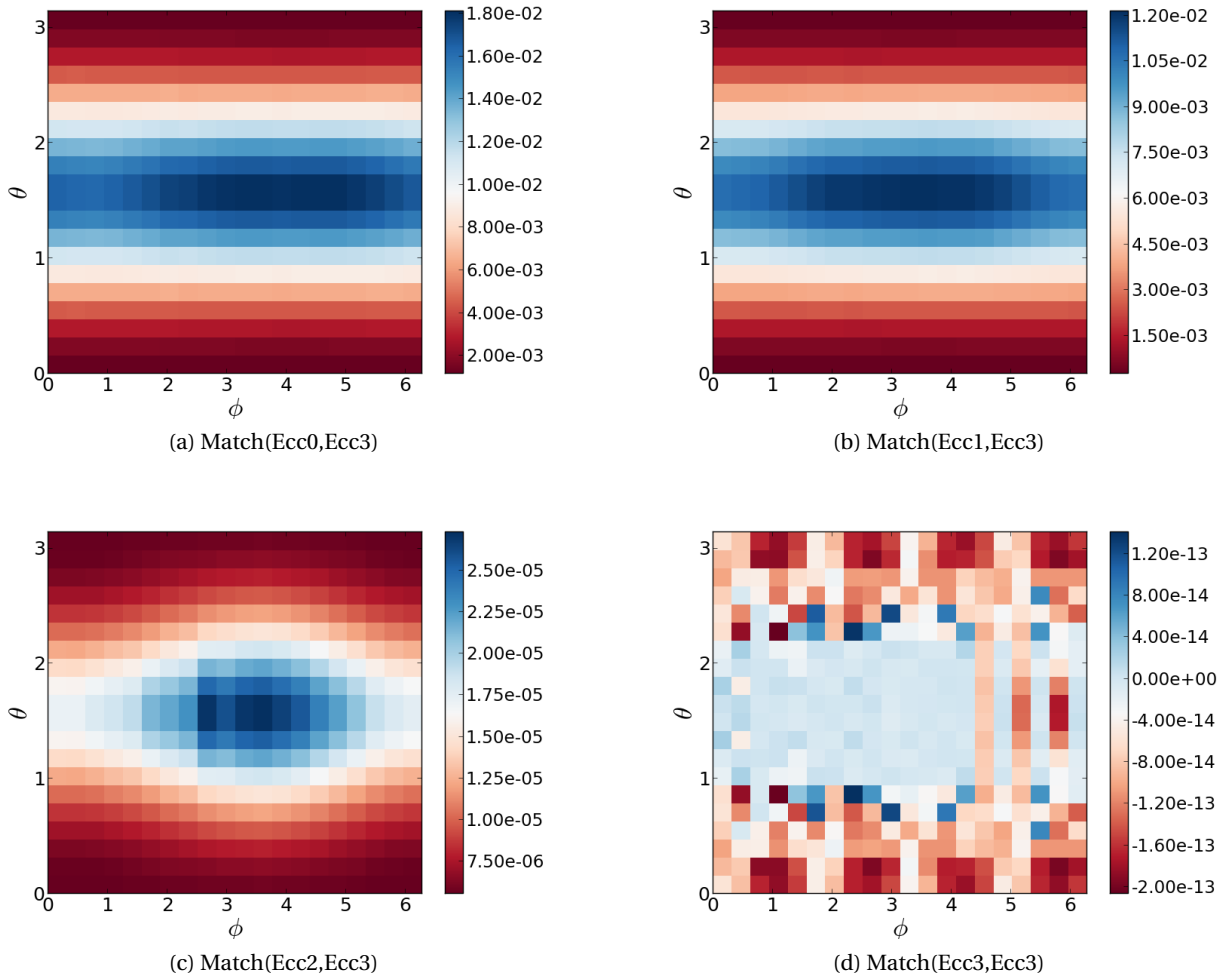

(a) Match(Ecc0,Ecc3)

(b) Match(Ecc1,Ecc3)

(c) Match(Ecc2,Ecc3)

(d) Match(Ecc3,Ecc3)

Figure 1: The GW mismatch ($mismatch = 1 - Match$) as a function of skyposition for the $(2,2)$ mode, for a flat noise power spectral density (PSD), or frequency independent noise. Note that the bottom right figure is a waveform compared to itself and is 0 to numerical precision, as expected.

is the least for BBHs orientated face-on. The maximum mismatch between waveforms from two non-spinning, $q = 3$, BBHs with $e = 0.0197$ and $e = 0.00628$ is 0.018. Also seen is the high dependence of mismatch on zenith angle, θ but not azimuthal angle, ϕ. However, in order to determine if a mismatch of 0.018 is significant with respect to other sources of mismatch, we also checked for the GW mismatch between:

- Lev5 vs. Lev4 waveforms. Since SpEC computes the same inspiral at multiple resolutions, comparing results from the highest resolution simulation (Lev5) and the second highest resolution simulation (Lev4) yields the GW mismatch due to discretization errors. We expect that any significant mismatch be above this magnitude. The maximum mismatch (over all propagation directions) was 0.00056 (figure 3 in Appendix)
- Ψ_4 (Weyl scalar) vs. $\ddot{h}_+ - i\ddot{h}_\times$. From the Newman-Penrose formalism, it can be shown that $\Psi_4 =$

$\ddot{h}_+ - i\ddot{h}_\times$. Since SpEC calculates h and Ψ_4 independently from each other, the mismatch between these waveforms provides lower limit for any computationally distinguishable mismatch. The maximum mismatch (over all propagations directions) was 0.000135 (figure 4 in Appendix).

3.3 Dependence on Observation Length

Figure 2 shows the total GW emission for face-on BBHs, Ecc3 and Ecc0. Although the two waveforms stay relatively in phase for the beginning inspiral, the more circular waveform merges first. The mismatch of the plotted waveforms is 0.0011.

In the future weeks, we will determine how small the eccentricity of a quasi-circular numerical BBH simulation must be for varying waveform lengths. For fewer observed cycles, we suspect that the tolerable eccentricity will increase, since the Match, as defined in equation 3.1 is a noise-weighted normalization, and not normalized over waveform length. This is particularly relevant because recent BBH observations in LIGO have varied significantly in length. Sources with larger masses can be seen for a few orbits (8 cycles from GW150914 [1]), whereas sources with smaller masses can be seen for many more orbits (55 cycles from GW151226 [11]).

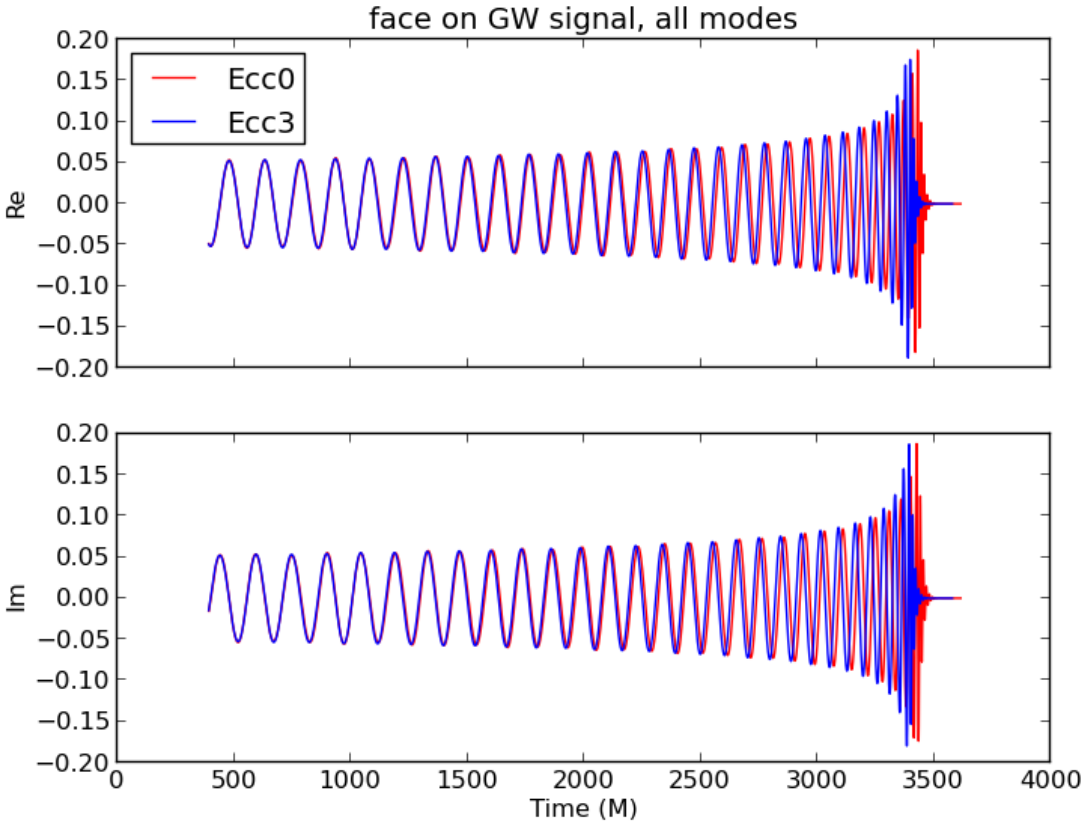

Figure 2: The real and imaginary amplitudes of the total GW emission for a non-spinning, face-on BBH of $q = 3$. The first $500M$ are omitted due to junk radiation.

REFERENCES

[1] B.P. Abbott et al., Phys. Rev. Lett. **116**, 061102 (2016).

[2] V. Tiwari et al., arXiv:1511.09240 (2015).

[3] `http://www.black-holes.org/SpEC.html`.

[4] L.T. Buchman, H.P. Pfeiffer, M.A. Scheel, and B. Szilágyi, Phys. Rev. D **86**, 084033 (2012).

[5] P. C. Peters and J. Mathews, Phys. Rev. **131**, 435 (1963).

[6] A.H. Mroué, M.A. Scheel, B. Szilágyi, et al., Phys. Rev. Lett. **111**, 241104 (2013).

[7] `http://www.black-holes.org/waveforms/`

[8] A. Buonanno et al., Phys. Rev. D **83**, 104034 (2011).

[9] A.H. Mroué, H.P. Pfeiffer, L.E. Kidder, and S.A. Teukolsky, Phys. Rev. D **82**, 124016 (2010).

[10] M. Boyle, Phys. Rev. D **87**, 104006 (2013)

[11] B.P. Abbott et al., Phys. Rev. Lett. **116**, 241103 (2016).

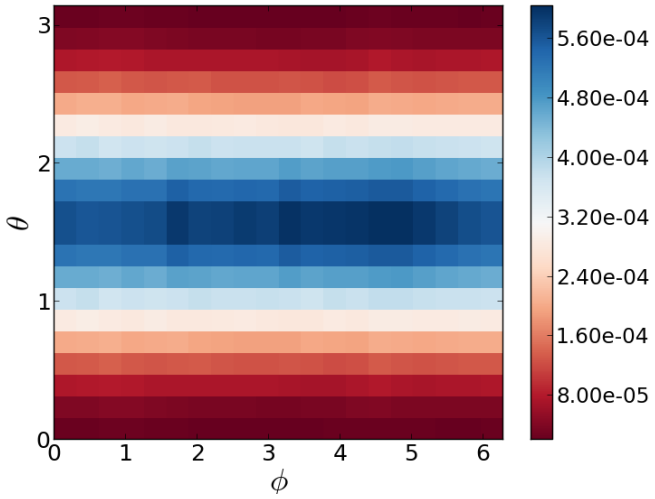

Figure 3: The GW mismatch as a function of propagation direction for the (2,2) mode, for a flat PSD, using the Ecc3 waveforms from the highest and second highest resolution runs.

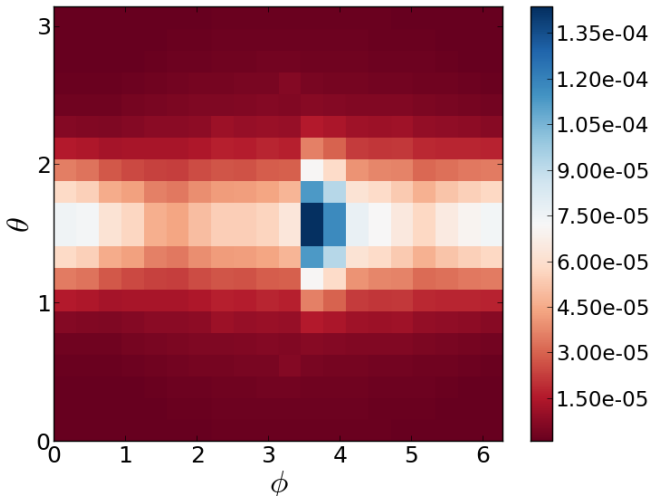

Figure 4: The GW mismatch as a function of propogation direction for the $(2,2)$ mode, for a flat PSD, which compares the independently calculated Weyl scalar Ψ_4 and the GW amplitude for Ecc0.